Available online at www.sciencedirect.com
ScienceDirect
Journal of Sound and Vibration 315 (2008) 467–485
JOURNAL OF SOUND AND VIBRATION
www.elsevier.com/locate/jsvi

System identification-guided basis selection for reduced-order nonlinear response analysis

Stephen A. Rizzi[a,*], Adam Przekop[b]

[a]NASA Langley Research Center, Structural Acoustics Branch, Hampton, VA 23681, USA
[b]National Institute of Aerospace, Hampton, VA 23666, USA

Accepted 19 December 2007
The peer review of this article was organised by the Guest Editor
Available online 14 February 2008

Abstract

Reduced-order nonlinear simulation is often times the only computationally efficient means of calculating the extended time response of large and complex structures under severe dynamic loading. This is because the structure may respond in a geometrically nonlinear manner, making the computational expense of direct numerical integration in physical degrees of freedom prohibitive. As for any type of modal reduction scheme, the quality of the reduced-order solution is dictated by the modal basis selection. The techniques for modal basis selection currently employed for nonlinear simulation are ad hoc and are strongly influenced by the analyst's subjective judgment. This work develops a reliable and rigorous procedure through which an efficient modal basis can be chosen. The method employs proper orthogonal decomposition to identify nonlinear system dynamics, and the modal assurance criterion to relate proper orthogonal modes to the normal modes that are eventually used as the basis functions. The method is successfully applied to the analysis of a planar beam and a shallow arch over a wide range of nonlinear dynamic response regimes. The error associated with the reduced-order simulation is quantified and related to the computational cost.
Published by Elsevier Ltd.

1. Introduction

Reduced-order finite element (FE)-based nonlinear simulation can be a very efficient means of calculating geometrically nonlinear static and dynamic response. Use of the FE method is required for analysis of complex aerospace structures, for which closed-form solutions are not available. The approach gets its computational advantage by reducing the size of the physical system using a nonlinear modal coordinate transformation. For large structural components, a reduction in system size by several orders of magnitude is possible [1]. In order to obtain an accurate reduced-order solution, an appropriate set of basis functions must be used in the nonlinear modal coordinate transformation. The selection of this set of basis functions, however, can be elusive for all but the simplest structures. Failure to select an appropriate basis can either lead

*Corresponding author. Tel.: +1 757 864 3599; fax: +1 757 864 8823.
E-mail address: stephen.a.rizzi@nasa.gov (S.A. Rizzi).

0022-460X/$ - see front matter Published by Elsevier Ltd.
doi:10.1016/j.jsv.2007.12.031

to inaccuracies in the reduced-order analysis, or to a large basis selection, which diminishes the computational advantage of the reduced-order analysis.

For the analysis of thin-walled structures, several approaches to modal basis selection have been offered in recent years. The most intuitive approach is to select normal modes (NMs), which are present in the excitation bandwidth. Such a basis has been shown to be insufficient, however, because it lacks the necessary nonlinear coupling between low- and high-frequency modes [2]. Further, attempts to select a small modal basis by exploiting structural or loading symmetry are misguided as doing so disallows anti-symmetric behaviors known to exist, for example, during snap-through events [3] and autoparametric resonance [4]. Some authors have successfully developed problem-specific displacement fields to serve as modal bases, including aeroelastic modes for the study of panel flutter [5], NMs obtained in the presence of thermal stress [6,7], NMs in combination with secondary fields [8,9], implicit condensation and expansion procedure (ICE) for in-plane basis modeling [10], and nonlinear modes [11]. While such bases can greatly reduce the system size at a particular loading condition, their application over a broad range of loading conditions may be problematic, necessitating a redefinition of the reduced-order system at different conditions. For the modal reduction process employed in this work, such redefinition can be accompanied by a significant computational penalty. Because of this penalty, the present authors have focused their efforts on selection of bases, which are not sensitive to the loading condition. They have demonstrated that bases consisting solely of NMs can yield reduced-order solutions, which are applicable over diverse nonlinear dynamic response regimes [2–4].

Regardless of the approach taken to select the basis, the accuracy of the reduced-order analysis must be determined. In the absence of closed-form solutions, this can be determined only through comparison with an alternative measure of the true response. For this purpose, experimental data [12–14] or a full-order FE analysis in physical degrees of freedom (dofs) are often employed [1–4,15]. Additional computational effort and/or expense are required in either case. For validation purposes however, only a short, but representative response time history is required, making comparison with a full-order analysis potentially more attractive. Once validated, the reduced-order analysis can be used to perform extended time simulations. Extended analyses are required in the case of random response to obtain statistically meaningful results [16]. Because a measure of the true response is needed for validating the reduced-order model, it can also guide the basis selection without incurring additional cost. The goal of this work is to develop a procedure for modal basis selection based on a system identification of the full-field nonlinear dynamic response.

A well-known and reliable procedure for system identification is proper orthogonal decomposition (POD) [17,18]. A review of POD applications to mechanical systems was recently provided by Kerschen et al. [19]. The procedure developed in this paper first performs a POD analysis to determine the proper orthogonal values (POVs) and proper orthogonal modes (POMs). The POVs are then used to determine the POMs with the greatest contribution [20,21]. Since POMs may change as the loading condition changes, they do not themselves form the preferred basis as the nonlinear modal transformation would potentially need to be repeated for each loading condition. Instead, a set of NMs which resembles a desired set of POMs is identified by employing the modal assurance criterion (MAC) [22]. Such an approach permits determination of a reduced-order system that remains applicable over a relatively large nonlinear response regime.

This paper re-examines two problems recently studied using a nonlinear reduced-order FE analysis; a planar beam [2,3] and a shallow arch [4] under various loading conditions. In these works, accurate reduced-order analyses were obtained using a modal basis obtained through engineering judgment without the aid of a formal procedure. It is shown that the POD/MAC procedure developed herein can be used to obtain comparable results while further reducing the size of the nonlinear system. When complemented by a metric to quantify error, the trade-off between the computational effort and accuracy of the reduced-order solution is established.

2. Formulation

The previously developed FE-based reduced-order nonlinear simulation is first summarized to illustrate the procedure for characterizing the nonlinear stiffness via an indirect evaluation procedure. The computational

effort associated with various elements of the reduced-order simulation procedure is discussed. Next, the POD procedure is discussed with consideration given to the partitioning of the correlation matrix for the problems under consideration. The participation of the POMs is computed using the POVs to ascertain the most significant POMs. These POMs are then related to NMs using the MAC. This set of NMs serves as the modal basis in the reduced-order nonlinear simulation.

2.1. Reduced-order nonlinear simulation

The equations of motion of the nonlinear system in the physical dofs may be written as

$$\mathbf{M}\ddot{\mathbf{x}}(t) + \mathbf{C}\dot{\mathbf{x}}(t) + \mathbf{f}_{\mathrm{NL}}(\mathbf{x}(t), \Delta T) = \mathbf{f}(t), \tag{1}$$

where $\mathbf{M}$ and $\mathbf{C}$ are the system mass and damping matrices, $\mathbf{x}$ is the displacement response vector, and $\mathbf{f}$ is the force excitation vector, respectively. The nonlinear restoring force $\mathbf{f}_{\mathrm{NL}}$ is a vector function dependent on $\mathbf{x}$ and the temperature increment ΔT, and generally includes linear, quadratic, and cubic stiffness terms.

A set of coupled modal equations with reduced dofs is first obtained by applying the modal coordinate transformation $\mathbf{x} = \mathbf{\Phi q}$ to Eq. (1), yielding the equation of motion in modal coordinates as

$$\tilde{\mathbf{M}}\,\ddot{\mathbf{q}}(t) + \tilde{\mathbf{C}}\,\dot{\mathbf{q}}(t) + \tilde{\mathbf{f}}_{\mathrm{NL}}(q_1(t), q_2(t), \ldots, q_L(t),\ \Delta T) = \tilde{\mathbf{f}}(t), \tag{2}$$

where $\mathbf{q}$ is the modal displacement response vector and $\mathbf{\Phi}$ is the modal basis matrix. When the basis consists of mass-normalized NMs, the system matrices in modal coordinates are expressed as

$$\tilde{\mathbf{M}} = \mathbf{\Phi}^{\mathrm{T}}\mathbf{M}\mathbf{\Phi} = \lceil \mathbf{I} \rfloor, \quad \tilde{\mathbf{C}} = \mathbf{\Phi}^{\mathrm{T}}\mathbf{C}\mathbf{\Phi} = \lceil 2\zeta_r\omega_r \rfloor, \quad \tilde{\mathbf{f}}_{\mathrm{NL}} = \mathbf{\Phi}^{\mathrm{T}}\mathbf{f}_{\mathrm{NL}}, \quad \tilde{\mathbf{f}} = \mathbf{\Phi}^{\mathrm{T}}\mathbf{f}, \tag{3}$$

where $\lceil\ \rfloor$ denotes a diagonal matrix, ω_r are the undamped natural frequencies, ζ_r are the viscous damping factors, and $r = 1, \ldots, L$, where L is the number of selected modes.

The analysis method employed in this work makes use of commercial FE programs to facilitate the study of complicated aerospace structures. The direct transformation of Eq. (1) to Eq. (2) requires knowledge of the system matrices and excitation vector. However, in the context of a commercial FE program, the nonlinear restoring force $\mathbf{f}_{\mathrm{NL}}$ is generally not known. Therefore, an indirect means of evaluating the nonlinear stiffness is applied [7,15]. The rth element of the nonlinear modal restoring force vector may be written in the form

$$\tilde{f}^{r}_{\mathrm{NL}}(q_1, \ldots, q_L, \Delta T) = \sum_{j=1}^{L} d^{r}_{j}(\Delta T)q_j + \sum_{j=1}^{L}\sum_{k=j}^{L} a^{r}_{jk}(\Delta T)q_j q_k + \sum_{j=1}^{L}\sum_{k=j}^{L}\sum_{l=k}^{L} b^{r}_{jkl}(\Delta T)q_j q_k q_l, \quad r = 1, \ldots, L, \tag{4}$$

where d, a, and b are the linear, quadratic nonlinear, and cubic nonlinear modal stiffness coefficients, respectively. The coefficients are obtained through a series of nonlinear static solutions using prescribed static displacement fields in physical coordinates. Each nonlinear static solution is performed using an implicit analysis. Expressing $\tilde{\mathbf{f}}_{\mathrm{NL}}$ in the form of Eq. (4) reduces the problem of determining the nonlinear stiffness from one in which a large set of simultaneous nonlinear equations must be solved to one involving simple algebraic relations.

The static displacement fields are formed from linear combinations of the basis functions. Scaling factors are applied to the basis functions such that the displacement fields have physically meaningful magnitudes. The process of evaluating the reduced-order stiffness terms was previously demonstrated to be insensitive to large variations in the scaling factor magnitude [15]. The number of nonlinear static solutions required depends on the number of modes selected and may be expressed as

$$\text{Number of solutions} = 3\binom{L}{1} + 3\binom{L}{2} + \binom{L}{3}, \quad L \geqslant 3, \tag{5}$$

where

$$\binom{L}{k} = \frac{L!}{k!(L-k)!} \tag{6}$$

is the number of combinations of k modes from the L selected modes. It is clear from Eq. (5) that the number of nonlinear static solutions increases nonlinearly with the number of included modes. Hence, there are several incentives for keeping the number of included modes to a minimum; the computational effort associated with the nonlinear stiffness evaluation procedure, that associated with integration of the coupled nonlinear system, and that associated with the inverse transformation. Fortunately, because the stiffness evaluation procedure is performed independent of the loading $\tilde{\mathbf{f}}(t)$, it need only be performed once *provided* that a suitable basis is chosen which fully characterizes the desired response regime. This consideration is particularly important for aerospace engineering problems, where structures may be exposed to a broad range of operating conditions.

Having determined the linear, quadratic nonlinear, and cubic nonlinear modal stiffness coefficients from the above procedure, the coupled modal nonlinear equations of motion in Eq. (2) are integrated using a fourth-order Runge–Kutta method. The resulting modal displacement time histories are transformed back to physical coordinates using the inverse modal transformation. The reduced-order analyses presented in this paper were performed with the ABAQUS [23] implementation of RANSTEP [24].

The cost of the nonlinear modal reduction can be regarded as a fixed computational cost, as the procedure has to be performed regardless of the amount of simulation time. By contrast, the cost of integrating Eq. (2) can be regarded as a variable cost, as it depends on the length of simulation time, which can vary significantly depending on the problem. Because of this, subsequent discussion regarding the computational cost is limited to the fixed cost associated with the nonlinear modal reduction.

2.2. System identification—proper orthogonal decomposition

The objective of the POD analysis is to identify the most significantly contributing POMs to the nonlinear dynamic response. The POD analysis employed in this study utilizes a short, but representative, record of the nonlinear dynamic displacement response obtained using a full-order FE analysis. If a single nonlinear stiffness evaluation is to be performed, it is imperative that this record capture all the nonlinear dynamics of interest. Therefore, an analysis of the most severe loading condition is typically sought. The full-field response $\mathbf{x}(t)$ is stored as a series of snapshots at discrete output times in the so-called snapshot matrix. The snapshot matrix is of size $n \times N$, where n is a number of the output time samples and N is the number of dofs. As subsequently discussed, the snapshot matrix may be partitioned into matrices that contain only a selected subset of dofs, e.g. only transverse displacements.

A correlation matrix $\mathbf{R}$ can be computed from the snapshot matrix as

$$\mathbf{R} = \frac{1}{n}\mathbf{X}^{\mathrm{T}}\mathbf{X}. \tag{7}$$

A correlation matrix computed from a full snapshot matrix is of size $N \times N$. An eigenanalysis of the correlation matrix is next performed, that is

$$[\mathbf{R} - \boldsymbol{\lambda}\mathbf{I}]\mathbf{p} = \mathbf{0} \tag{8}$$

to determine the vector of POVs ($\boldsymbol{\lambda}$) and the $N \times N$ matrix of POMs,

$$\mathbf{P} = [\mathbf{p}_1 \;\; \mathbf{p}_2 \ldots \mathbf{p}_N]. \tag{9}$$

Each POM vector $\mathbf{p}$ is fully populated due to the nonlinear coupling inherent in the nonlinear analysis from which the snapshot matrix is obtained. The POVs are a measure of the modal activity, and the POMs are the dominant vibration shapes of the structure. The higher the POV, the greater the contribution of the corresponding POM to the response. POMs obtained for an undamped linear system would be identical to the NMs of the system. The difference between the NMs and POMs increases with increasing damping and nonlinearity [20,21].

The POM participation factor, χ_i, is a measure of the participation of the ith POM and is determined from the expression:

$$\chi_i = \frac{\lambda_i}{\sum_{j=1}^{N}\lambda_j}, \quad i = 1, \ldots, N. \tag{10}$$

The sum of all POM participation factors is unity. The cumulative POM participation factor, υ, of a selected subset of POMs, defined as

$$\upsilon = \sum_{i=1}^{M} \chi_i, \quad 0 < \upsilon \leqslant 1, \tag{11}$$

where M is a number of selected POMs, i.e. $M < N$. The cumulative participation factor is used to determine the number of rank-ordered POMs needed to achieve a prescribed value.

2.3. Modal basis selection

For simple structures the process of matching POMs with NMs resembling their shapes can be quite straightforward and does not require a quantitative metric. The relationship between POMs and NMs becomes more difficult to establish, however, as the complexity of a structure and the number of dofs increases. Therefore, a more robust approach is required. A good measure of the similarity of two vectors is the MAC [22]. For a pair of POM $\mathbf{p}$ and NM $\boldsymbol{\varphi}$ vectors, the MAC value can be obtained from

$$\mathrm{MAC}(\mathbf{p}_k, \phi_l) = \frac{|\mathbf{p}_k^{\mathrm{T}} \boldsymbol{\varphi}_l|^2}{(\mathbf{p}_k^{\mathrm{T}} \mathbf{p}_k)(\boldsymbol{\varphi}_l^{\mathrm{T}} \boldsymbol{\varphi}_l)}, \quad \begin{matrix} k = 1, \ldots, M, \\ l = 1, \ldots, N. \end{matrix} \tag{12}$$

Computation of MAC values for every pair of selected POMs and NMs enables identification of strongly correlated pairs. The POD analysis establishes which POMs are required for a specified cumulative participation. Once these POMs are identified, the NMs most closely resembling them are determined via their MAC value. This collection of NMs forms the modal basis.

2.3.1. Special conditions for linearly uncoupled/weakly coupled systems

There exists a special set of conditions under which modification of the above POD/MAC procedure is beneficial. These conditions exist when the modes can be characterized as being transverse-dominated or in-plane dominated. This is the case, for example, for flat isotropic structures and structures with shallow curvature. Low-frequency, transverse-dominated modes are those modes for which the maximum amplitude of the transverse displacement component is much larger than the maximum amplitude of the in-plane displacement component. High-frequency, in-plane dominated modes are those modes for which the maximum amplitude of the in-plane displacement component is much larger than the maximum amplitude of the transverse displacement component. The POM matrix, on the other hand, is always fully populated. Consequently, there is an inherent mismatch between NMs and POMs. To handle this condition, the snapshot matrix may be partitioned to contain only a single dof type. There are as many snapshot matrices, and hence correlation matrices, as there are dofs per node. For example, in the case of a beam having three dofs per node, the snapshot matrix would be partitioned into three matrices; one for transverse displacements, one for in-plane displacements, and one for rotations. This modification reduces the size of each snapshot matrix to $n \times m$, and the size of each correlation matrix to $m \times m$, where m is the number of nodes. The eigenanalysis of the each correlation matrix, determination of participation factors for each dof, and MAC analysis are subsequently performed independent of one another. In this case, the set of all N partitioned NMs in the MAC analysis contain only a single dof each.

Finally, for the above conditions, the rotational dofs and the transverse displacement dofs are not independent. Separate POD/MAC analyses of these dofs would therefore identify the same NMs. To avoid this redundancy, only the transverse displacement dofs and in-plane displacement dofs are analyzed in the following sections.

3. Results

The reduced-order analysis of two previously considered structures was revisited to demonstrate the efficacy of the POD/MAC procedure for modal basis selection. The planar isotropic beam [2,3] was first studied to validate the proposition that a basis consisting of a single set of NMs is applicable over a wide range of loading

conditions. The shallow arch [4] was next studied to demonstrate that the procedure used to partition the snapshot matrix is valid for structures with modes that have weak linear coupling, i.e. modes that have non-zero in-plane displacements for the transverse-dominated modes, and non-zero transverse displacements for the in-plane-dominated modes.

3.1. Planar beam

The beam under investigation measured $457.2 \times 25.4 \times 2.286$ mm ($l \times w \times h$), and had clamped boundary conditions at both ends. Material properties for aluminum were used: Young's modulus $E = 73.11$ GPa, shear modulus $G = 27.59$ GPa, mass density $\rho = 2763\,\mathrm{kg/m^3}$, and coefficient of thermal expansion $\alpha = 22.32\,(\mu\mathrm{m/m})/^{\circ}\mathrm{C}$. A fixed modal damping value of 14.52 1/s was used, giving a 2% critical damping for the first symmetric transverse mode at 57.8 Hz.

The FE model of the beam consisted of 144 ABAQUS B21 beam elements, each measuring 3.175 mm long. The B21 Timoshenko beam element uses linear interpolation functions and a lumped mass formulation. The element has one mid-span integration point and two nodes, each with two translational and one rotational dofs. Therefore, for the 145 node (m) model, the total number of dofs (N) was 435. Clamped boundary conditions were modeled by constraining all three dofs at both ends of the beam, reducing the active number of dofs to 429.

The POD/MAC analysis was performed to select a modal basis using full-order analysis results from a strongly nonlinear response regime induced by combined thermal-acoustic loading. To demonstrate the robustness of the modal basis so derived, analyses using this same basis were performed for a similar, but less severe loading condition, for an acoustic loading condition having no thermal component, and finally for a dynamic thermal buckling condition with no acoustic loading.

3.1.1. POD/MAC-based modal basis selection for the planar beam

The full-order nonlinear response of the beam was analyzed in physical dofs with the ABAQUS [23] FE code. The ABAQUS/Explicit solution was used with an automatic time step adjustment, known as 'element-by-element' in ABAQUS. This approach yields a conservative time step increment.

The beam was simultaneously subjected to a uniformly distributed random pressure loading and a uniform temperature increment. A band-limited white noise random pressure time history was generated by summing equal amplitude sine waves, each with random phase, at a frequency resolution of 0.61 Hz in the frequency range 0–1500 Hz [25]. An overall sound pressure level (OASPL) of 170 dB (re: 20 μPa) was applied. The steady-state temperature increment of 19.44 °C exceeded the critical buckling temperature increment of 3.67 °C. This loading condition resulted in a strongly nonlinear response exhibiting persistent snap-through behavior [3]. The total simulation time was 2.1384 s, however the initial 0.5 s was removed to provide 1.6384 s of fully developed response for the subsequent POD/MAC analysis. A total of 32,768 data points (n) at an output sampling of 50 μs were utilized in the POD/MAC analysis. Five ensemble averages were taken to generate the response power spectral densities (PSDs) that follow. Each PSD presented has a frequency resolution of 0.61 Hz.

The POD analysis was performed individually on the partitioned transverse displacement and in-plane displacement snapshot matrices. POM/MAC data for the first 12 transverse POMs is presented in Table 1. Shown are the POV participation factor computed per Eq. (10), the cumulative POV participation factor computed per Eq. (11), the corresponding NM as determined by the MAC analysis, the NM natural frequency, and the MAC values computed per Eq. (12). The NM number was assigned in order of ascending natural frequency. The same quantities for the first 12 in-plane POMs are listed in Table 2. Note that the cumulative POVs in Tables 1 and 2 are rounded to the nearest one-hundredth. It is seen that the cumulative POV factor converges faster for the transverse POMs than it does for the in-plane POMs. It is also seen that the MAC values for the transverse NMs are generally higher than they are for the in-plane NMs.

Given the relatively high values of the MAC for both transverse and in-plane modal components, there was no need to represent a single POM with multiple NMs. The selection of a modal basis for the reduced-order analysis was therefore based exclusively on identifying the POMs above some threshold value of the

Table 1
Transverse POVs for the beam under a 170 dB/19.44 °C thermal-acoustic loading

POM number	POV (%)	Cumulative POV (%)	NM number	NM natural frequency (Hz)	MAC
1	85.39	85.39	1	57.817	0.998
2	10.68	96.07	2	159.34	0.999
3	3.10	99.17	3	312.29	0.998
4	0.52	99.69	4	516.05	0.999
5	0.25	99.94	5	770.56	1.000
6	0.03	99.97	7	1431.3	1.000
7	0.02	99.99	6	1075.7	0.999
8	0.001	99.99	8	1837.3	0.996
9	0.0006	99.99	9	2293.3	0.987
10	0.00003	99.99	10	2799.3	0.892
11	0.000002	99.99	11	3354.9	0.770
12	0.000001	99.99	12	3960.0	0.686

Table 2
In-plane POVs for the beam under a 170 dB/19.44 °C thermal-acoustic loading

POM number	POV (%)	Cumulative POV (%)	NM number	NM natural frequency (Hz)	MAC
1	68.99	68.99	15	5625	0.974
2	18.59	87.58	22	11,250	0.962
3	4.62	92.20	28	16,874	0.861
4	4.51	96.71	33	22,495	0.990
5	1.40	98.11	38	28,114	0.721
6	1.14	99.25	42	33,729	0.944
7	0.38	99.63	51	44,947	0.641
8	0.25	99.88	47	39,340	0.930
9	0.07	99.95	58	56,144	0.880
10	0.04	99.99	54	50,548	0.582
11	0.01	100.0	65	67,313	0.846
12	0.004	100.0	62	61,732	0.582

cumulative POV factor. The same cumulative POV threshold of $\upsilon > 99.99\%$ was chosen for both in-plane and transverse displacement components. This resulted in identification of a modal basis consisting of 17 NMs (7 transverse and 10 in-plane). In the subsequent reduced-order analysis results that follow, an additional modal basis consisting of 24 NMs (the 12 transverse and 12 in-plane modes presented in Tables 1 and 2) was considered. This basis was previously examined by the authors without the aid of the POD/MAC procedure [3].

Since the POD/MAC modal basis selection was performed at the 170 dB/19.44 °C loading condition, good agreement between the reduced- and full-order analyses are expected at this condition. Transverse and in-plane displacement PSDs obtained from the reduced-order analyses at the quarter-span location are presented in Figs. 1 and 2, respectively. The quarter-span location was chosen because it does not precisely coincide with nodal points of selected transverse and in-plane NMs. The mid-span location on the other hand is at a nodal point for every other transverse and in-plane NM due to symmetry. Excellent agreement is noted across the frequency range. It is seen that there is no substantial difference in the quality of the results obtained with the 17-mode basis identified using the POD/MAC procedure and results obtained with the 24-mode basis previously considered. However, the fixed computational cost, as indicated by Eq. (5), is more than 2.5 times greater for the 24-mode basis than it is for the 17-mode basis (2924 vs. 1139 static nonlinear cases). Thus, while the POD/MAC procedure did not improve the quality of the reduced-order results, it identified a modal basis having a substantially reduced computational cost.

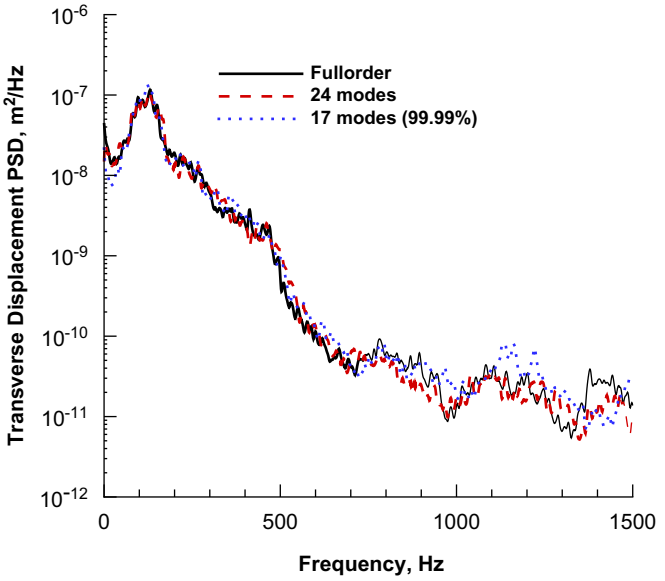

Fig. 1. Quarter-span transverse displacement PSD at the 170 dB/19.44 °C loading condition.

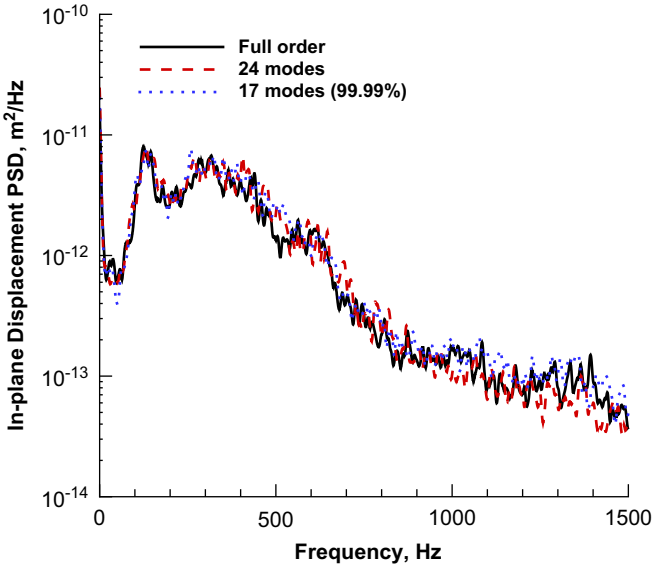

Fig. 2. Quarter-span in-plane displacement PSD at the 170 dB/19.44 °C loading condition.

3.1.2. Robustness Study 1—Nonlinear response at a reduced thermal-acoustic loading condition

The previously selected modal basis consisting of 17 modes was applied to a less severe acoustic loading of 158 dB and the same temperature increment of 19.44 °C. This loading condition resulted in an intermittent snap-through response. To broaden the scope of the investigation, additional bases were considered having cumulative POV threshold values of 90.00%, resulting in a selection of 5 modes (2 transverse and 3 in-plane modes), 99.00%, resulting in a selection of 9 modes (3 transverse + 6 in-plane modes), and 99.90%, resulting in a selection of 14 modes (5 transverse + 9 in-plane modes). The 24-mode basis was also retained.

The PSDs comparing the reduced-order solutions with the full-order analysis solution are presented in Figs. 3 and 4, for transverse and in-plane displacements at the quarter-span, respectively. It is seen that the

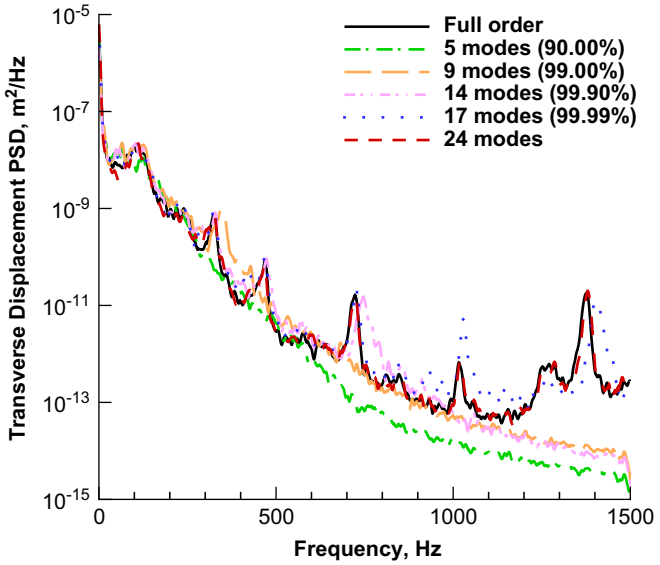

Fig. 3. Quarter-span transverse displacement PSD at the 158 dB/19.44 °C loading condition.

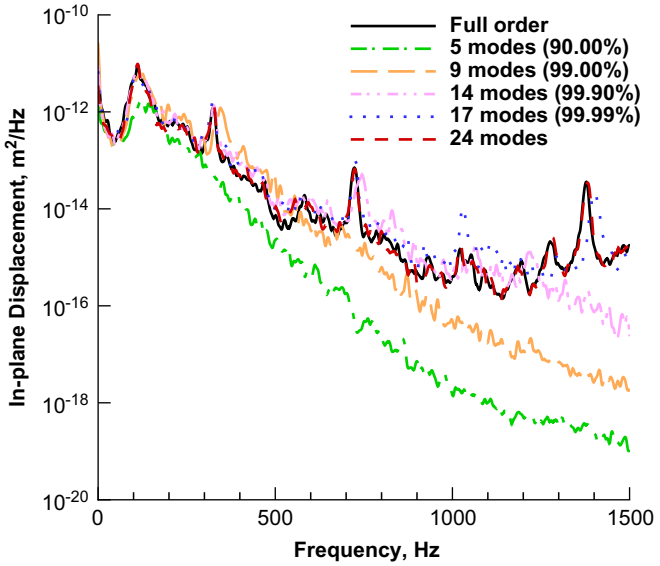

Fig. 4. Quarter-span in-plane displacement PSD at the 158 dB/19.44 °C loading condition.

PSD comparison improves as additional modes are added to the basis. Because the excitation spectrum is flat, the lower frequency NMs contribute more to the displacement response than the higher frequency modes. Improvements to the solution are thus more noticeable at the higher frequencies as the modal basis is expanded. However, improvement of the peak magnitudes, broadening characteristics, and frequencies are apparent in the lower frequency range as well. Figs. 5 and 6 present a measure of the error as a function of frequency between the reduced-order analyses and the full-order analysis. The error is computed as the ratio of the full-order analysis solution to the reduced-order solution at each frequency. For the 5-mode basis, the error in the in-plane displacement (Fig. 6) is greater that that of the transverse displacement (Fig. 5). However, as the basis is expanded, both reduced-order in-plane and transverse displacement components achieve a comparable, and small, amount of error relative to the full-order analysis solution.

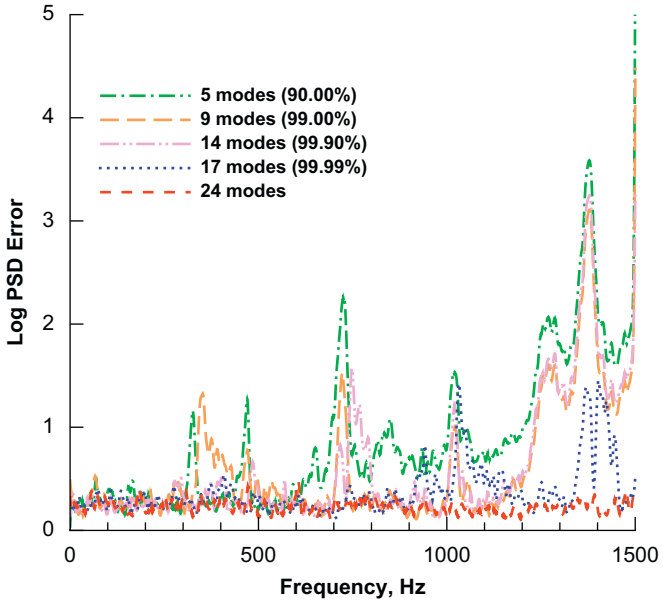

Fig. 5. Quarter-span transverse displacement error at the 158 dB/19.44 °C loading condition.

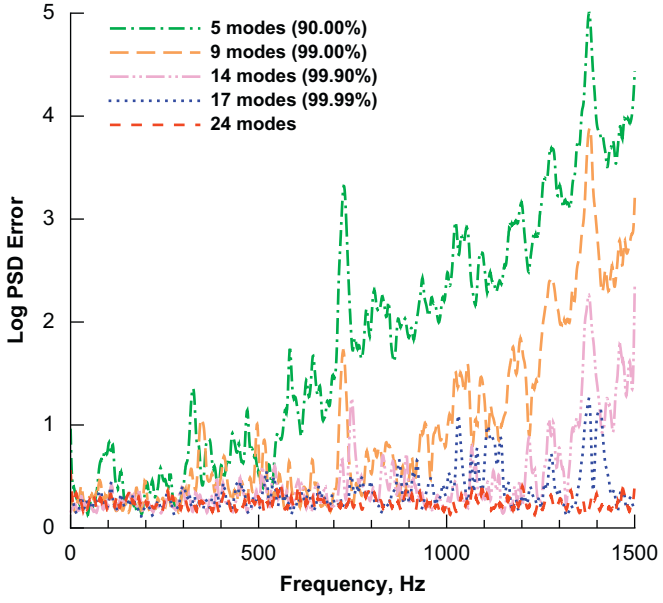

Fig. 6. Quarter-span in-plane displacement error at the 158 dB/19.44 °C loading condition.

A compact measure of the error presented in Figs. 5 and 6 can be obtained as the integral of all the frequency component errors. This integrated metric is plotted in Fig. 7 as a function of the size of the modal basis for the transverse and in-plane displacement components. The number of nonlinear static cases needed to perform the nonlinear modal reduction, per Eq. (5), is also shown. The computational expense associated with error reduction is clearly seen. Both the error and the computational cost of modal reduction are nonlinear functions of the number of NMs included in the basis. As the error approaches the asymptote, the computational expense grows more rapidly.

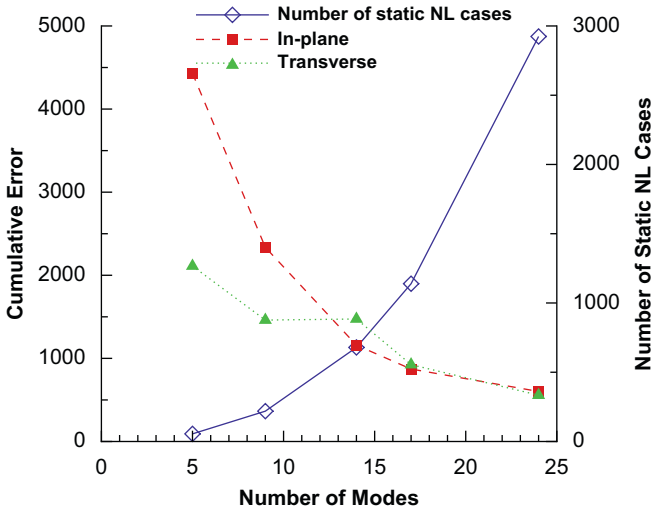

Fig. 7. Quarter-span integrated in-plane displacement error at the 158 dB/19.44 °C loading condition.

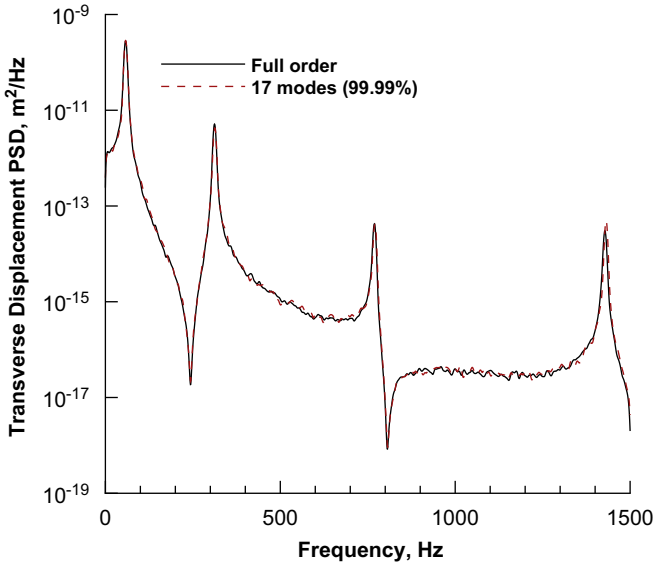

Fig. 8. Quarter-span transverse displacement PSD at the 128 dB ambient temperature loading condition.

The behavior in the transverse displacement error in Fig. 7 warrants additional discussion. An almost flat characteristic is noted between the 9- and the 14-mode bases. The cumulative POV criterion used in the modal basis selection is developed from the response at all locations, while the results shown in Fig. 7 were obtained at a chosen quarter-span location. The two transverse NMs needed to expand the 9-mode basis to the 14-mode basis do not significantly contribute to the response at the quarter-span location. In the limit, NMs that have a nodal point at the location on the structure where the physical displacement is recovered do not contribute to the response at all.

3.1.3. Robustness Study 2—Linear response to acoustic loading

In this study, a substantial reduction in the acoustic loading to 128 dB and a complete elimination of the thermal load results in a small amplitude unbuckled response. The quarter-span transverse and in-plane displacement PSDs obtained using the previously identified 17-mode basis are shown in Figs. 8 and 9,

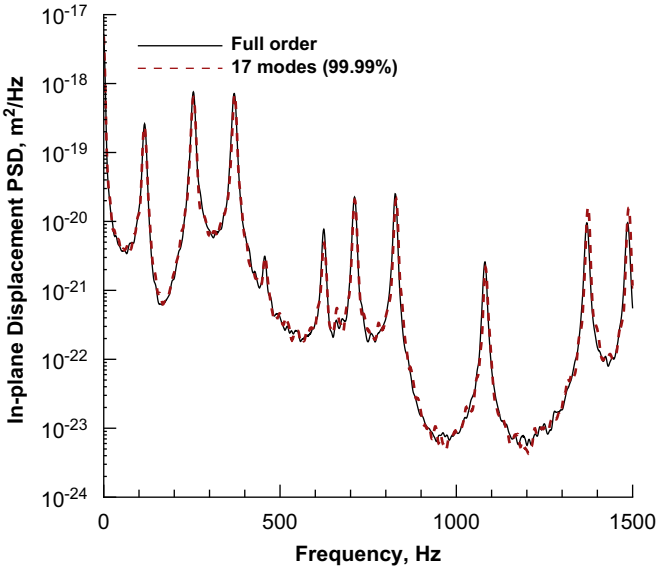

Fig. 9. Quarter-span in-plane displacement PSD at the 128 dB ambient temperature loading condition.

respectively. Both show excellent agreement with the full-order analysis results. It was previously found that anti-symmetric transverse and symmetric in-plane modes identified during snap-through events are not excited at this loading condition and do not contribute to the overall response [3]. Therefore, some of the computational efficiency is lost in the time integration portion of the reduced-order analysis using the 17-mode basis. However, the fact that the modal reduction procedure does not have to be repeated represents a computational savings and added convenience. It also highlights the fact that a modal basis expanded beyond the point of some desired accuracy will not negatively affect the computed response.

3.1.4. Robustness Study 3—Dynamic thermal buckling analysis

The last study considers the beam instantaneously subjected to the originally applied temperature increment of 19.44 °C, but with no random acoustic loading. For the idealized FE model with no imperfections, application of thermal loading exceeding the critical buckling temperature will not cause the beam to buckle. A small initial perturbation is needed to trigger the loss of stability. In the present analysis, this disturbance is provided by a small force temporarily applied in the transverse direction at the mid-span node, as described in Ref. [3]. Once the loss of stability is triggered, the beam undergoes a single dynamic thermal buckling event and the unforced damped oscillations eventually stabilize about one of the two thermally buckled equilibriums.

The time history response of such an event for the transverse and in-plane displacement components are shown in Figs. 10 and 11, respectively. The top plot in both figures presents the quarter-span location results and the bottom plot in each figure presents the mid-span location results. The decaying response for the full-order solution and the 17- and 24-mode reduced-order solutions compare very well throughout the entire event. Particularly noteworthy is how well the reduced-order analyses capture the delayed in-plane displacement response at the mid-span location, as seen in the bottom plot of Fig. 11.

A point-by-point error metric is not considered appropriate for the transient analysis as differences in the time history response are expected. Even two full-order nonlinear analyses, one using an explicit integration scheme and the other an implicit scheme, will differ in this regard due to the manner in which the nonlinear stiffness is handled. Consequently, the reduced-order analysis, having its nonlinear stiffness derived from full-order nonlinear implicit analyses, and the full-order explicit analysis will likewise differ. A qualitative comparison is therefore considered more appropriate. Such comparative analysis is sufficient to identify solutions obtained using a deficient basis, as shown in Fig. 12 for a 12-mode solution of the same

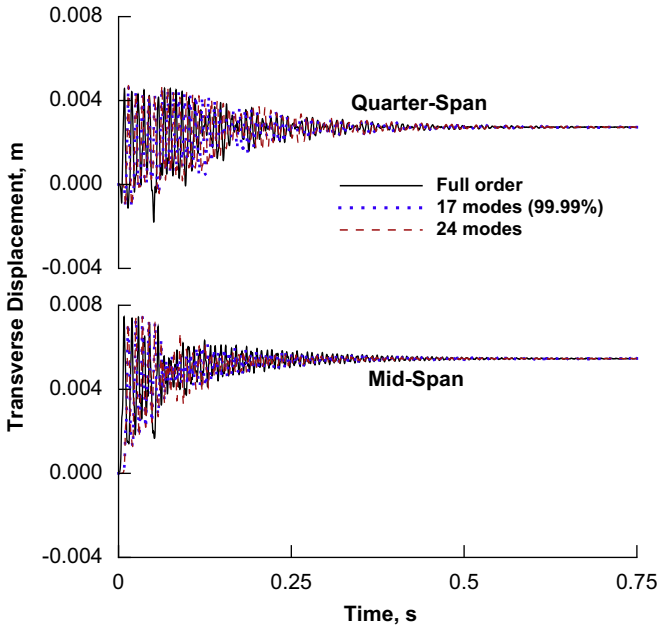

Fig. 10. Transverse displacement time history during a single dynamic snap-through event.

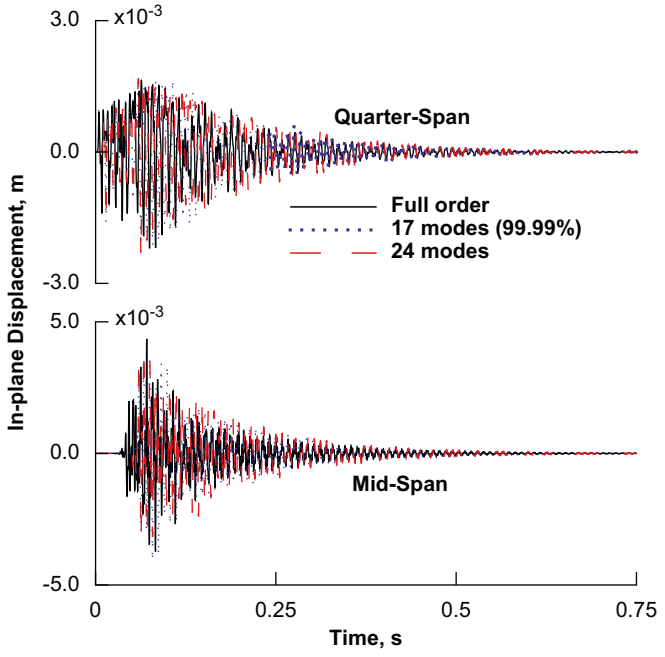

Fig. 11. In-plane displacement time history during a single dynamic snap-through event.

snap-through event. This 12-mode basis, consisting of NMs 1, 3, 5, 7, 9, 11, 22, 33, 42, 51, 58, and 65 (see Tables 1 and 2), is a subset of the 24-mode basis used above.

The above results effectively validate the proposition that a basis consisting of a single set of well-chosen NMs is applicable over a wide range of loading conditions. This conclusion is important as it relates to practical application of the reduced-order analysis method. For example, a single modal basis may be used in

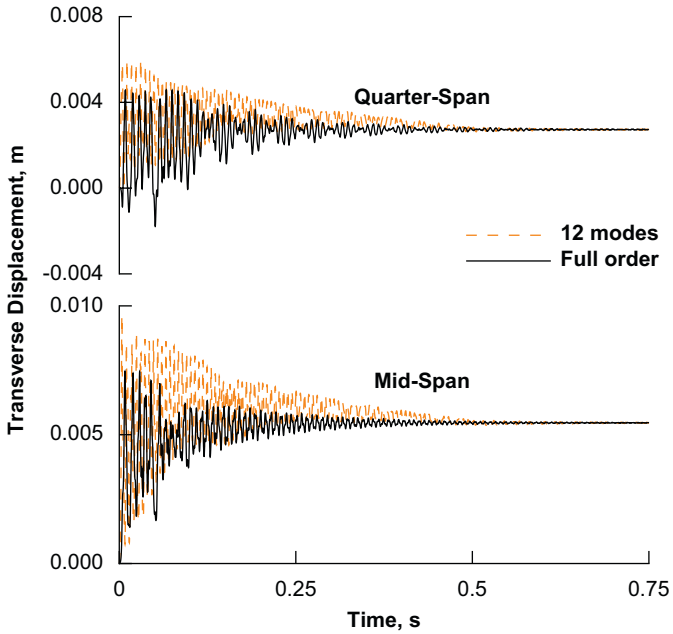

Fig. 12. Transverse displacement time history during a single dynamic snap-through event obtained using a deficient basis.

the design and analysis of extreme flight regime vehicle structures, including hypersonic planes or launch vehicles, where operating conditions change drastically.

3.2. Shallow arch

Having demonstrated the efficacy of the POD/MAC analysis, and the partitioning of the snapshot matrix for a flat isotropic structure, the analysis of the shallow arch is next undertaken to demonstrate the validity of the partitioning procedure for structures having weak linear coupling. The arch measured $457.2 \times 25.4 \times 2.286$ mm ($l \times w \times h$, where l is the projected length), and had clamped boundary conditions at both ends. The cylindrical curvature had a radius of 2063.75 mm, resulting in a mid-span rise of 12.7 mm. The same aluminum material properties utilized in the planar beam study were used for the arch, except for the damping. For the arch, a fixed modal damping value of 64.88 1/s was used, giving a 2% critical damping for the first symmetric transverse (transverse-dominated) mode at 258.2 Hz. Note that the fundamental mode for this structure is the first anti-symmetric transverse (transverse-dominated) mode at 158.3 Hz. The FE model of the arch used the same discretization of 144 ABAQUS B21 beam elements as the planar beam problem. Clamped boundary conditions were also modeled in the same fashion.

3.2.1. POD/MAC-based modal basis selection for the shallow arch

The POD/MAC analysis was performed using results from ABAQUS/Explicit. The arch was subjected to a vertical uniformly distributed random loading of 114.13 N/m, having a flat spectrum over the frequency range 0–1500 Hz. This loading condition resulted in a highly nonlinear response exhibiting intermittent autoparametric behavior [4]. Under autoparametric conditions, the response amplitude dramatically increases and the modal participation became richer relative to non-autoparametric condition. The simulation time, output sampling, and PSD post-processing parameters used were identical to those used in the planar beam study.

The response snapshot matrix was partitioned into two matrices; one containing transverse displacement dofs and one containing in-plane displacement dofs. As in the case of the beam, the rotational dofs and the transverse displacement dofs are not independent and were therefore not treated separately in the POD/MAC analysis. Table 3 presents data for the first 12 transverse POMs. Shown are the POV participation factor

Table 3
Transverse POVs for the shallow arch under a 114.3 N/m distributed vertical loading

POM number	POV (%)	Cumulative POV (%)	NM number	NM natural frequency (Hz)	MAC
1	35.61	35.61	2	258.17	0.560
2	33.92	69.53	1	158.25	0.777
3	26.48	96.01	3	400.41	0.730
4	2.73	98.74	5	773.72	1.000
5	1.09	99.83	4	513.19	1.000
6	0.16	99.99	7	1426.0	1.000
7	0.008	100.0	6	1070.1	0.996
8	0.0006	100.0	9	2282.7	0.958
9	0.0002	100.0	8	1828.0	0.971
10	0.00002	100.0	11	3339.0	0.754
11	0.00001	100.0	10	2785.4	0.785
12	0.000001	100.0	13	4592.1	0.324

Table 4
In-plane POVs for the shallow arch under a 114.3 N/m distributed vertical loading

POM number	POV (%)	Cumulative POV (%)	NM number	NM natural frequency (Hz)	MAC
1	66.48	66.48	15	5624	0.956
2	29.29	95.76	22	11,225	0.904
3	3.03	98.80	33	22,437	0.797
4	0.84	99.64	28	16,831	0.830
5	0.21	99.85	42	33,638	0.791
6	0.08	99.93	38	28,039	0.768
7	0.06	99.99	51	44,826	0.969
8	0.01	100.0	47	39,235	0.733
9	0.003	100.0	58	55,991	0.867
10	0.001	100.0	65	67,130	0.532
11	0.001	100.0	54	50,411	0.541
12	0.0001	100.0	62	61,564	0.920

computed per Eq. (10), the cumulative POV participation factor computed per Eq. (11), the corresponding NM number as determined by the MAC analysis, the NM natural frequency, and the MAC values computed per Eq. (12). The NM number was assigned in order of ascending natural frequency. Table 4 presents the same quantities for the first 12 in-plane POMs.

Recall for the beam that both the transverse and in-plane displacement components were dominated by a single in-plane POM corresponding to the lowest transverse and in-plane NMs, respectively. A similar characteristic is noted in the in-plane response of the arch, as seen in the first entry in Table 4. However, this characteristic is not found in the transverse response of the arch, where the first three transverse POMs have comparable contributions ranging from 26% to 36%, as seen in Table 3. The presence of the second POM, corresponding to the first anti-symmetric transverse mode at 158.3 Hz, is due to the intermittent autoparametric behavior indicated at this loading condition [4]. It is also observed that these three transverse POMs are less correlated with the first three NMs than in the case of the beam. This is evidenced by their reduced MAC values; compare MAC values of the beam of nearly unity with those of the arch ranging from 0.56 to 0.78. The behavior is partly attributable to the higher level of damping applied in the shallow arch analysis compared to that applied in the beam analysis. It is known that the POM and NM shapes, while identical in the undamped linear response regime, depart from each other as the damping increases [20,21].

Like the beam, a cumulative POV threshold value of 99.99% was chosen for both the transverse and in-plane POMs. This resulted in selection of 13 POMs (6 transverse displacement and 7 in-plane displacement

POMs), and consequently in selection of 13 corresponding NMs (6 transverse displacement dominated and 7 in-plane displacement dominated). From the earlier study [4], a second modal basis consisting of 16 NMs (the 8 lowest transverse displacement dominated and the 8 lowest in-plane displacement dominated) was additionally considered.

The resulting transverse and in-plane displacement PSDs at the mid-span location for the 114.13 N/m reference excitation case are shown in Figs. 13 and 14, respectively. Excellent agreement of the 13- and 16-mode bases reduced-order results with the full-order solution is observed in Fig. 13 for the transverse displacement component. Good agreement is also noted in Fig. 14 for the in-plane displacement component, with the most significant differences three orders of magnitude below the peak response. The 13-mode nonlinear modal reduction requires solution of 559 static nonlinear cases while the 16-mode reduction requires

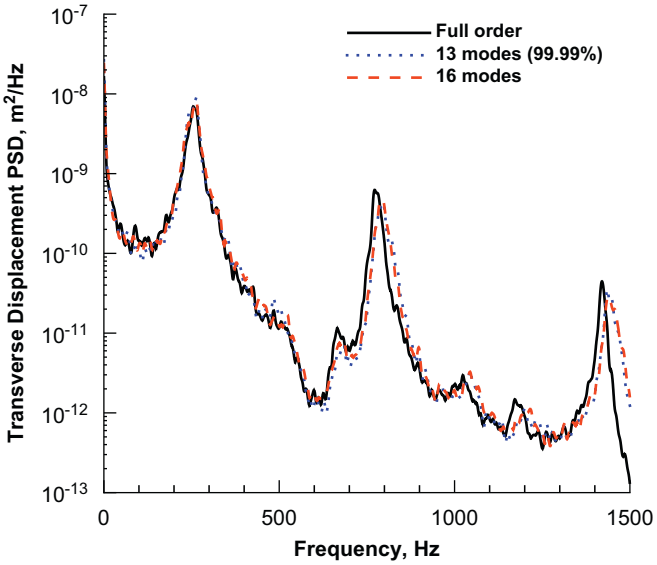

Fig. 13. Mid-span transverse displacement PSD at the 114.3 N/m loading condition.

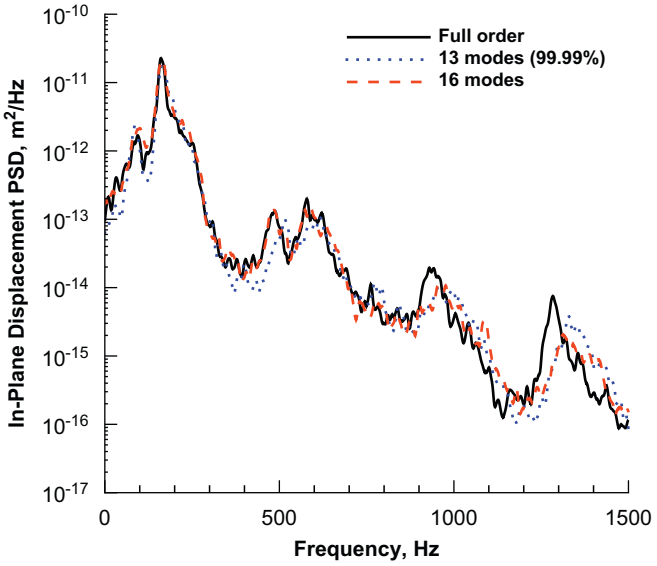

Fig. 14. Mid-span in-plane displacement PSD at the 114.3 N/m loading condition.

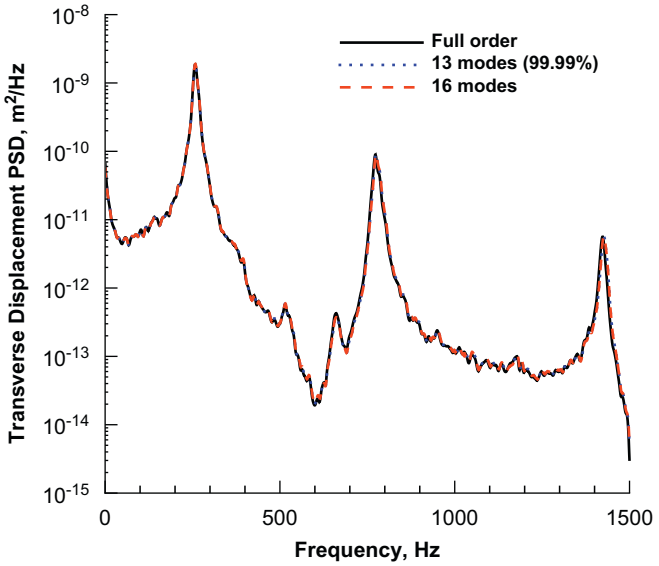

Fig. 15. Mid-span transverse displacement PSD at the 40.35 N/m loading condition.

968 cases. The 73% increase in computational cost amounts to little appreciable improvement in the quality of results. Hence, application of POD/MAC procedure provided a smaller modal basis selection than was found without such guidance, while effectively preserving the same high quality of the results.

3.2.2. Robustness Study 4—Nonlinear response at a reduced loading condition

The purpose of this last investigation is to further demonstrate the broad range of loading conditions over which a well-chosen NM basis is applicable. The 13-mode basis identified above was used in a reduced-order analysis to predict the response of the arch under a reduced loading condition that produced a slightly nonlinear response without autoparametric behavior. The 16-mode basis was also kept for comparison. Fig. 15 presents the transverse displacement PSD at the mid-span location at a loading level of 40.35 N/m. Excellent agreement between both reduced- and the full-order solutions is found. Because autoparametric behavior is not indicated at this response level, the in-plane displacement along the span of the arch is entirely anti-symmetric in character, i.e. the in-plane displacement at the mid-span location is zero.

The results obtained for the shallow arch prove that partitioning of the transverse and in-plane dofs in the POD/MAC procedure is a valid strategy for structures with weak linear coupling, and leads to selection of an efficient modal basis.

4. Conclusions

A procedure for selecting an efficient modal basis for use in a nonlinear reduced-order analysis of structures undergoing geometrically nonlinear dynamic response has been developed. The procedure requires a short, representative sample of the full-field nonlinear dynamic response. A POD analysis of this response is performed, and resulting POMs are correlated to linear NMs using the modal assurance criteria. Reduced-order nonlinear simulation results were found to accurately predict the response and an integrated error metric between the reduced-order and full-order analyses was found to monotonically decrease as the modal basis was expanded. Consideration of the error metric together with a computational cost function helps enable a greater understanding of the trade-off between accuracy and computational effort.

It was also demonstrated that a single basis consisting only of NMs can be used over a wide range of loading conditions, provided that the POD/MAC procedure used to identify those modes is performed with suitable sample data. For this purpose, analysis of the most severe loading condition was performed so that all the nonlinearities could be exercised. Identification of a single normal modal basis offers computational

advantages because the nonlinear modal transformation need only be performed once. This makes the current analysis well-suited for aerospace applications where loading conditions may vary significantly across flight regimes. As alluded to in robustness study 2, additional computational savings could be realized for more benign loading conditions by adaptively reducing the basis obtained under the most severe loading condition to a smaller basis. This benefit would come in the integration stage and could be achieved by considering the modal participation from a short duration reduced-order simulation, without the need for an additional POD/MAC analysis and nonlinear stiffness evaluation.

For thin-walled structures with weak or no linear coupling, it was found that the POD/MAC analysis could be performed independently on the transverse and in-plane displacement responses. Further development of the methodology is required for application to more complicated two- and three-dimensional aerospace structures, which require larger FE models, have greater modal density, and exhibit a greater degree of linear coupling.

References

[1] A. Przekop, S.A. Rizzi, D.S. Groen, Nonlinear acoustic response of an aircraft fuselage sidewall structure by a reduced-order analysis, in: M.J. Brennan, S.L. Liguore, B.R. Mace, J.M. Muggleton, K.D. Murphy, B.A.T. Petersson, S.A. Rizzi, R. Shen (Eds.), *Structural Dynamics: Recent Advances, Proceedings of the Ninth International Conference*, Paper 135, The Institute of Sound and Vibration Research, University of Southampton, Southampton, UK, 2006.

[2] S.A. Rizzi, A. Przekop, The effect of basis selection on static and random acoustic response using a nonlinear modal simulation, Technical Paper NASA/TP-2005-213943, NASA Langley Research Center, Hampton, VA, December 2005.

[3] A. Przekop, S.A. Rizzi, Dynamic snap-through of thin-walled structures by a reduced-order method, *AIAA Journal* 45 (10) (2007) 2510–2519.

[4] A. Przekop, S.A. Rizzi, Nonlinear reduced order finite element analysis of structures with shallow curvature, *AIAA Journal* 44 (8) (2006) 1767–1778.

[5] X. Guo, C. Mei, Using aeroelastic modes for nonlinear panel flutter at arbitrary supersonic yawed angle, *AIAA Journal* 41 (2) (2005) 272–279.

[6] X. Guo, A. Przekop, C. Mei, Y.Y. Lee, Thermal buckling suppression of supersonic vehicle surface panels using shape memory alloy, *Journal of Aircraft* 41 (6) (2004) 1498–1504.

[7] M.P. Mignolet, A.G. Radu, X. Gao, Validation of reduced order modeling for the prediction of the response and fatigue life of panels subjected to thermo-acoustic effects, in: M.J. Brennan, M.A. Ferman, B.A.T. Petersson, S.A. Rizzi, K. Wentz (Eds.), *Structural Dynamics: Recent Advances, Proceedings of the Eighth International Conference*, The Institute of Sound and Vibration Research, University of Southampton, Southampton, UK, 2003.

[8] P. Tiso, E. Jansen, A finite element based reduction method for nonlinear dynamics of structures, *Proceedings of the 46th AIAA/ASME/ASCE/AHS/ASC Structures, Structural Dynamics, and Materials Conference*, AIAA-2005-1867, Austin, TX, 2005.

[9] P. Tiso, E. Jansen, M. Abdalla, A reduction method for finite element nonlinear dynamic analysis of shells, *Proceedings of the 47th AIAA/ASME/ASCE/AHS/ASC Structures, Structural Dynamics, and Materials Conference*, AIAA-2006-1746, Newport, RI, 2006.

[10] J.J. Hollkamp, R.W. Gordon, Modeling membrane displacements in the sonic fatigue response prediction problem, *Proceedings of the 46th AIAA/ASME/ASCE/AHS/ASC Structures, Structural Dynamics and Materials Conference*, AIAA-2005-2095, Austin, TX, 2005.

[11] R. Arquier, S. Bellizzi, B. Cochelin, Computation of nonlinear modes of elastic structures, *EUROMECH Colloquium 483-Geometrically Non-linear Vibrations of Structures*, Porto, Portugal, July 2007, pp. 287–290.

[12] T.J. Beberniss, R.W. Gordon, J.J. Hollkamp, The effect of air on the nonlinear response of a plate, *Proceedings of the 48th AIAA/ASME/ASCE/AHS/ASC Structures, Structural Dynamics, and Materials Conference*, AIAA-2007-2085, Honolulu, HI, April 2007.

[13] J.J. Hollkamp, T.J. Beberniss, R.W. Gordon, The nonlinear response of a plate to acoustic loading: predictions and experiments, *Proceedings of the 47th AIAA/ASME/ASCE/AHS/ASC Structures, Structural Dynamics & Materials Conference*, AIAA-2006-1928, Newport, RI, 2006.

[14] J.J. Hollkamp, R.W. Gordon, S.M. Spottswood, Nonlinear sonic fatigue response prediction from finite element modal models: a comparison with experiments, *Proceedings of the 44th AIAA/ASME/ASCE/AHS/ASC Structures, Structural Dynamics, and Materials Conference*, AIAA-2003-1709, Norfolk, VA, 2003.

[15] A.A. Muravyov, S.A. Rizzi, Determination of nonlinear stiffness with application to random vibration of geometrically nonlinear structures, *Computers and Structures* 81 (15) (2003) 1513–1523.

[16] S.M. Spottswood, H.F. Wolfe, D.L. Brown, The effect of record length on determining the cumulative damage of ceramic matrix composite beam, in: N.S. Ferguson, H.F. Wolfe, M.A. Ferman, S.A. Rizzi (Eds.), *Structural Dynamics: Recent Advances, Proceedings of the Seventh International Conference*, Southampton, UK, 2000, pp. 785–799.

[17] O. Nelles, *Nonlinear System Identification*, Springer, Berlin, 2001.

[18] D.J. Ewins, *Modal Testing: Theory and Practice*, Research Studies Press Ltd., Hertfordshire, 2000.

[19] G. Kerschen, J.-C. Golinval, A.F. Vakakis, L.A. Bergman, The method of proper orthogonal decomposition for dynamical characterization and order reduction of mechanical systems: an overview, *Nonlinear Dynamics* 41 (1–3) (2005) 147–169.
[20] B.F. Feeny, R. Kappagantu, On the physical interpretation of proper orthogonal modes in vibrations, *Journal of Sound and Vibration* 211 (4) (1998) 607–616.
[21] B.F. Feeny, On proper orthogonal co-ordinates as indicators of modal activity, *Journal of Sound and Vibration* 255 (5) (2002) 805–817.
[22] R.J. Allemang, D.L. Brown, A correlation coefficient for modal vector analysis, *Proceedings of International Modal Conference*, 1982, pp. 110–116.
[23] ABAQUS version 6.6 On-line Documentation, *ABAQUS Analysis User's Manual*, Abaqus, Inc., Providence, RI, 2005 (Section 6.3.3).
[24] S.A. Rizzi, A. Przekop, Estimation of sonic fatigue by reduced-order finite element based analysis, *Structural Dynamics: Recent Advances, Proceedings of the 9th International Conference*, The Institute of Sound and Vibration Research, University of Southampton, Southampton, UK, July 2006.
[25] S.A. Rizzi, A.A. Muravyov, Comparison of nonlinear random response using equivalent linearization and numerical simulation, in: N.S. Ferguson, H.F. Wolfe, M.A. Ferman, S.A. Rizzi (Eds.), *Structural Dynamics: Recent Advances, Proceedings of the Seventh International Conference*, Vol. 2, The Institute of Sound and Vibration Research, University of Southampton, Southampton, UK, 2000, pp. 833–846.